Epidermal Growth Factor Receptor (EGFR) Density May Not Be the Only Determinant for the Efficacy of EGFR-Targeted Photoimmunotherapy in Human Head and Neck Cancer Cell Lines

Wei Peng,[1,2] Henriette S. de Bruijn,[2] Eric Farrell,[3] Mouldy Sioud,[4] Vida Mashayekhi,[5] Sabrina Oliveira,[5,6] Go M. van Dam,[7] Jan L. N. Roodenburg,[1] Max J. H. Witjes,[1*] and Dominic J. Robinson[2]

[1]Department of Oral and Maxillofacial Surgery, University of Groningen, University Medical Center Groningen, Groningen, The Netherlands

[2]Department of Otorhinolaryngology and Head and Neck Surgery, Center for Optical Diagnostics and Therapy, Erasmus Medical Center, Rotterdam, The Netherlands

[3]Department of Oral and Maxillofacial Surgery, Special Dental Care and Orthodontics, Erasmus Medical Center, Rotterdam, The Netherlands

[4]Department of Cancer Immunology, Institute for Cancer Research, Oslo University Hospital-Radiumhospitalet, Oslo, Norway

[5]Cell Biology, Science Faculty, Department of Biology, Utrecht University, Utrecht, The Netherlands

[6]Pharmaceutics, Science Faculty, Department of Pharmaceutical Sciences, Utrecht University, Utrecht, The Netherlands

[7]Department of Surgery, Nuclear Medicine and Molecular Imaging and Intensive Care, University of Groningen, University Medical Center Groningen, Groningen, The Netherlands

Objective: The aim of this study was to investigate the effects of targeted photoimmunotherapy (PIT) *in vitro* on cell lines with various expression levels of epidermal growth factor receptor (EGFR) using an anti-EGFR targeted conjugate composed of Cetuximab and IR700DX, phthalocyanine dye.

Materials and Methods: Relative EGFR density and cell binding assay was conducted in three human head & neck cancer cell lines (scc-U2, scc-U8, and OSC19) and one reference cell line A431. After incubation with the conjugate for 1 or 24 hours, cellular uptake and localization were investigated by confocal laser scanning microscopy and quantified by image analysis. Cell survival was determined using the MTS assay and alamarBlue assay after PIT with a 690 nm laser to a dose of 7 $J.cm^{-2}$ (at 5 $mW.cm^{-2}$). The mode of cell death was examined with flow cytometry using apoptosis/necrosis staining by Annexin V/propidium iodide, together with immunoblots of anti-apoptotic Bcl-2 family proteins Bcl-2 and Bcl-xL.

Results: A431 cells had the highest EGFR density followed by OSC19, and then scc-U2 and scc-U8. The conjugates were localized both on the surface and in the cytosol of the cells after 1- and 24-hour incubation. After 24-hour incubation the granular pattern was more pronounced and in a similar pattern of a lysosomal probe, suggesting that the uptake of conjugates by cells was via receptor-mediated endocytosis. The results obtained from the quantitative imaging analysis correlate with the level of EGFR expression. Targeted PIT killed scc-U8 and A431 cells efficiently; while scc-U2 and OSC19 were less sensitive to this treatment, despite having similar EGFR density, uptake and localization pattern. Scc-U2 cells showed less apoptotic cell dealth than in A431 after 24-hour targeted PIT. Immunoblots showed significantly higher expression of anti-apoptotic Bcl-2 and Bcl-xL proteins in scc-U2 cell lines compared to scc-U8.

Conclusion: Our study suggests that the effectiveness of EGFR targeted PIT is not only dependent upon EGFR density. Intrinsic biological properties of tumor cell lines also play a role in determining the efficacy of targeted PIT. We have shown that in scc-U2 cells this difference may be caused by differences in the apoptopic pathway. Lasers Surg. Med. 50:513–522, 2018. © 2018 Wiley Periodicals, Inc.

Key words: epidermal growth factor receptor; photoimmunotherapy; Cetuximab-IR700DX conjugate; head and neck cancer

INTRODUCTION

Photodynamic therapy (PDT) of cancer is based on the local or systemic administration of a photosensitizer

Conflict of Interest Disclosures: All authors have completed and submitted the ICMJE Form for Disclosure of Potential Conflicts of Interest and none were reported.

*Correspondence to: Max J. H. Witjes, MD, DDS, PhD, Department of Oral and Maxillofacial, University Medical Center Groningen, Hanzeplein 1, P.O. Box 30.001, 9700 RB Groningen, The Netherlands. E-mail: m.j.h.witjes@umcg.nl

Accepted 10 April 2018
Published online 19 May 2018 in Wiley Online Library (wileyonlinelibrary.com).
DOI 10.1002/lsm.22930

followed by activation with visible light of a specific wavelength. The light-activated photosensitizer transfers the energy to molecular oxygen to produce highly cytotoxic reactive oxygen species (ROS), notably singlet oxygen, resulting in photodamage to tumor cells/tissues [1–3]. A photosensitizer is, however, generally not selectively taken up by tumor cells [4] which can lead to significant damage to surrounding normal cells.

To overcome this limitation, targeted photoimmunotherapy (PIT) first reported by Mew et al., in 1983 [5], involves the conjugation of a photosensitizer to an antibody that specifically targets a protein on the surface of tumor cells. Such conjugates have the potential for effective photosensitizer delivery to cause selective destruction of individual cancer cells after light irradiation. Cetuximab-IR700DX is a conjugate of a phthalocyanine dye and an antibody against human epidermal growth factor receptor (EGFR). IR700DX has a strong absorption in the red (690 nm) wavelength where the light penetration into tissue is close to optimal. However, as a single agent IR700DX has very little photodynamically active because it is highly water soluble and does not localize close to essential organelles [6]. EGFR is highly expressed in many types of tumors including head and neck squamous cell carcinoma. This conjugate is currently under investigation for clinical use [7].

PIT efficacy using a different conjugate has previously been demonstrated in the human squamous cell carcinoma cell line A431 and MDAMB468-luc adenocarcinoma cell line *in vitro* [6]. Both cell lines strongly over-express EGFR. Furthermore, destruction of tumor xenografts in mice has also been demonstrated after PIT [7,8]. EGFR targeted PIT using nanobody conjugates has shown a positive relationship between EGFR expression and efficacy in EGFR over-expressing cell lines of A431 and UM-SCC-14C, whereas the Hela tumor cells with a low EGFR expression were spared [9].

The efficacy of cell death in PDT is mainly determined by the subcellular sites where a photosensitizer is located and therefore where singlet oxygen is generated. For targeted photosensitizers that are initially localized at the cell membrane this causes mainly necrosis by disruption of the cell membrane [9]. In addition, intracellular located photosensitizer can induce various pathways of apoptosis (programmed cell death), such as up regulation of p53 or cytochrome C. Apoptosis is a form of cell death that is morphologically and biochemically distinct from necrosis [10,11], and can be categorized into early and late stages. Early apoptosis is characterized by an intact plasma membrane with the exposure of phosphatidylserine on the cell surface; while late apoptosis is characterized by a permeable plasma membrane [12]. Stress on various organelles of cells including the mitochondria, endoplasmic reticulum (ER), endo/lysosomes, and nucleus can initiate specific apoptotic pathways [13–15]. During apoptosis, Bcl-2 family proteins regulate apoptotic process including anti-apoptotic members such as Bcl-2 and Bcl-xL and pro-apoptotic members such as BAX and BAD [16,17]. Previous reports have shown that both Bcl-2 and Bcl-xL proteins induced the resistance of tumor cells to PDT [18].

It has previously been shown that the effectiveness of targeted EGFR therapies depends upon the cellular density of EGFR [9,19]. The aim of this study was to investigate targeted PIT responses using Cetuximab-IR700DX in the human head and neck squamous cell carcinoma cell lines, scc-U8, scc-U2, and OSC19. We studied the EGFR expression, microscopic localization, cell survival, and mode of cell death after PIT using 1 or 24 hours of incubation. The 1 hour short drug light interval was chosen to aim for memebrane localized conjugate/EGFR receptor targeted responses; whereas the 24 hours incubation was to mimic a clinical scenario of using the conjugate.

MATERIALS AND METHODS

Chemicals—Cetuximab-IR700DX Conjugate

IR700DX is a phthalocyanine-type photosensitizer; while Cetuximab is a clinically used antibody against human EGFR. The conjugate was provided by Aspyrian Therapeutics, Inc., San Diego, CA.

Cell Lines

Three human head and neck (oral cavity) squamous cell carcinoma cell lines, scc-U8, scc-U2 (University of Michigan), and OSC19 (University of Leiden); and one human cervical squamous cell carcinoma cell line, A431 (University of Oslo) as a reference, were used in this study. The A431, scc-U8, and scc-U2 cell lines were cultured in Dulbecco's Modified Eagle Medium (DMEM, Gibco, Invitrogen, UK) supplemented with 10% foetal calf serum (FCS), 100 Uml^{-1} penicillin, 100 μgml^{-1} streptomycin, and 2 mM glutamine (PAA, Germany) at 37°C in a humidified 5% CO_2 atmosphere. The OSC19 cell line was cultured in DMEM (Invitrogen, Carlsbad, CA) containing 4.5 g D-glucoseL^{-1}, 110 mgl^{-1} sodium pyruvateL^{-1}, 580 mg L-glutamineL^{-1} supplemented with 10% FCS (Lonza, Basel, Switzerland), 400 $IUml^{-1}$ penicillin, 100 $\mu g/ml^{-1}$ streptomycin (Invitrogen), 1 × Minimal Essential Medium (MEM) non-essential amino acids solution and 1 × MEM vitamin solution at 37°C in a humidified 5% CO_2 atmosphere. The passages of 10–40 of the cell lines were used in this study.

Relative EGFR Expression and Conjugate Binding

Since IR700DX is a fluorescent dye, it is possible to directly detect IR700DX fluorescent signals of the conjugates to study cellular EGFR expression. Cells of each cell line were incubated with Cetuximab-IR700DX conjugates at the concentration of 40 μgml^{-1} (approx. 263.8 $nmolml^{-1}$) for 30 min at 4°C before being prepared for flow cytometry. This concentration was calculated to be sufficient to saturate all the EGFR receptors on the A431 cell line, based on data from a previous study [20]. The mean fluorescence intensity was used to measure the relative human EGFR expression in various cell lines. Cells without the conjugate were measured as background

signals. In addition a cell binding assay was conducted. For each cell line 8,000 cells was seeded in a 96-well plate (Nunc, Roskilde, Denmark). After 24-hour incubation for attachment, the plates were kept at 4°C and cells were washed with cold DMEM binding medium containing 1% BSA and 25 mM HEPES without phenol red at pH 7.4. After incubation of cells with Cetuximab-IR700DX conjugates (100–0.39 nM, 1:2 serial dilution) for 2-hours at 4°C, unbound conjugate was washed away three times with binding buffer. The amount of bound conjugate was detected with Odyssey Infrared scanner using the 700 nm channel. Fluorescence intensities were plotted (in triplicate ± SD) versus the concentrations using the GraphPad Prism 7 software (GraphPad Software, San Diego, CA).

Cell Survival

Cell proliferation was assessed with a standard MTS kit (CellTiter 96® AQueous One Solution Reagent (Promega Corp., Madison, WI) according to the manufacturer's recommendations using a 96-well plate reader (Molecular Devices, Sunnyvale, CA). It is a colorimetric method based on the cellular conversion of a tetrazolium compound into a formazan product, which can be detected by the 492 nm absorbance. Such absorbance measurements were not influenced by IR700DX. Cell viability was assessed with a standard alamarBlue Assay (alamarBlue™ Cell Viability Reagent) according to the manufacturer's protocol using a 96-well plate reader (Molecular Devices, Sunnyvale, CA). It is a fluorescent method based on a non-fluorescent molecule resazurin converting to a fluorescent molecule resorufin by reduction reactions in the cytoplasma of metabolically active cells, which can be measured at 590 nm. Such fluorescence measurements were not influenced by IR700DX.

Dark Cytotoxicity of Cetuximab and Cetuximab-IR700DX Conjugates

A total of 15,000 cells of each cell line were seeded per well in a 96-well plate. After attachment for 24-hours, the cells were incubated with various concentrations (up to 2,000 μgml^{-1}) Cetuximab and (from 10 μgm^{l-1} to 2,000 μgml^{-1}) of Cetuximab-IR700DX conjugates in the dark for 24-hours. The cell proliferation was then evaluated by the MTS assay.

Subcellular Localization of Cetuximab-IR700DX Conjugates and Quantitative Image Analysis

A total of 25,0000 cells of each cell line were seeded on the 0.25 $mgml^{-1}$ poly-lysine coated 24-mm cover slides and incubated in 10% FCS DMEM medium containing 40 μgml^{-1} of Cetuximab-IR700DX conjugates for 1- or 24-hour incubation. The cells were washed with medium once before being placed in a temperature-controlled 37°C mini incubator (Peecon, Germany). The subcellular localization of fluorescent conjugates was imaged using the dual-channel Zeiss LSM 510–Axiovert 200M (Carl Zeiss, Thornwood, NY) confocal microscopy (40×/1.3NA Plan-neofluar oil objective) with an excitation wavelength of 633 and a 650 nm long-pass emission filter. The cells were optically sectioned and 10 groups of cells at two different optical sections (z-stack) were randomly chosen in each cell line with various incubation times to quantify the fluorescent intensities of conjugates at three various locations of the cytoplasm membrane, endo/lysosomes, and cytosol of cells by the Fiji ImageJ software package.

PIT Treatment Protocols

Each cell line was seeded with 15,000 cells in each well of a 96-well plate. After 24-hour incubation for attachment, the cells were incubated in the dark with various concentrations of Cetuximab-IR700DX conjugates from 10 to 100 μgml^{-1} for 1- or 24-hour at 37°C. The cells were then washed with medium once and a volume of 100 µl medium was added in each well before being illuminated with a 690 nm laser (Modulight ML7700, Finland) using a shaker with a speed of 700 RPM to introduce a constant amount of oxygen into the medium during irradiation. We measured the fluence rate to be constant across all of the illuminated wells using an isotropic detector placed in the plane of the cells. The light dose of 7 $J.cm^{-2}$ at a fluence rate of 5 $mW.cm^{-2}$ (22 minutes) were used in the experiments because our previous study showed that these treatment parameters were effective at killing A431 cells and did not induce any hyperthermal effects [21]. Twenty-four hours after PIT cell survival was determind with both cell proliferation MTS assay and cell viability AlamarBlue assay. Since previous reports from us and others have shown very little photodynamic effect on cells using IR700DX alone, we chose not to include it as a control [6,9].

Mode of Cell Death

The mode of cell death after PIT was studied in the A431 and scc-U2 cell lines by flow cytometry using the commercial kit (VPS Diagnostics, Hoeven, the Netherlands) of Annexin V/propidium iodide to detect apoptosis and necrosis. The samples were prepared according to the manufacturer's instruction. Samples were analyzed using a BD FACS Jazz (BD, Erembodigem, Belgium) and FlowJo V10.0.8 (FlowJo LLC). Cells positive for annexin V only are considered in early apoptosis, while cells positive for PI only are considered necrotic. Cells that are positive for both Annexin V and PI are considered in late apoptosis or secondary necrosis.

Western Blots

Protein extracts (40 µg/lane) of scc-U2 and scc-U8 from whole-cell samples were separated by electrophoresis on 10% SDS–PAGE and then electro-transferred to nitrocellulose membranes. After blocking in 5% milk in TBS buffer (0.1% Tween) for 2-hour, the membranes were incubated overnight at 4°C with rabbit polyclonal IgG antibodies against Bcl-2, Bcl-xL or beta actin in TBS buffer (all from Santa Cruz, Heidelberg, Germany). After washing the membranes were incubated with HRP-conjugated anti-rabbit IgG. ECL detection reagent was used to visualize the reactive bands. Finally, the Western blot signals were quantified using the ChemiDoc XRS digital imaging system.

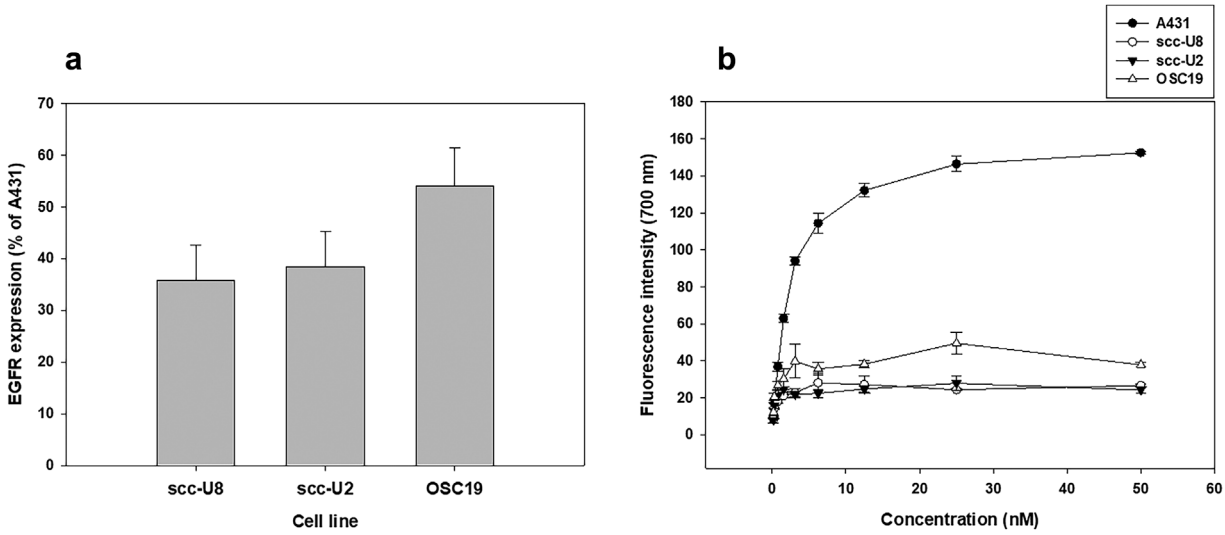

Fig. 1. EGFR expression in the scc-U8, scc-U2, and OSC19 cell lines, measured with flow cytometry (The data are presented as the percentages of EGFR expression of the A431 cells where the errorbars are calculated from the full width at half maximum [FWHM] of the fluorescence signal) (**a**) and cell binding assay (**b**).

Statistical Analysis

The results were analyzed (SigmaPlot®12; Sysat software, Inc.) using the unpaired Student *t*-test for data with normal distribution; otherwise, the Wilcoxon signed rank test was used. The differences were considered statistically significant with P value <0.05.

RESULTS

EGFR Expression and Conjugate Binding in Various Cell Lines

Figure 1a shows various amounts of EGFR expression determined using flow cytometry in scc-U8, scc-U2, and OSC19 cell lines after incubation with the conjugates at $40\,\mu g ml^{-1}$ for 30 min at 4°C. The EGFR expression in different head and neck cell lines is presented relative to the EGFR expression in the A431 cells (set to 100%): 36% in scc-U8, 38% in scc-U2, and 54% in OSC19; respectively. The scc-U8 and scc-U2 had a similar level of EGFR expression; while OSC19 expressed a slightly higher EGFR level. All three head and neck tumor cell lines had a much lower EGFR expression than the A431 cell line. Figure 1b shows the conjugate binding to A431, scc-U8, scc-U2, and OSC19 cell lines. The fluorescence intensity detected at saturating levels (i.e., where a plateau is observed) is in agreement with the EGFR expression levels determined using flow cytometry. The binding affinity (K_d) was similar for the three head and neck cell lines (Table 1).

Intracellular Localization of Cetuximab-IR700DX Conjugates

After 1-hour incubation the fluorescence of Cetuximab-IR700DX was observed on the cell membranes as well as in a granular pattern within the cells, particularly in A431 cells. After 24-hour incubation, the granular pattern of the conjugates became more pronounced in all cell lines (Fig. 2a). Co-incubation with an endo/lysosomal probe showed a similar pattern as seen in yellow overlap (Fig. 2b), suggesting that the conjugates were taken up through the endo/lysosomal pathway.

Quantitative Image Analysis

After 1-hour incubation conjugates were localized on the cell membrane and in the endo/lysosomes with significantly higher fluorescence signals in both locations in A431 cells than other cell lines ($P < 0.05$). Low fluorescence signals of the conjugates were seen in the cytosol in all cell lines (Fig. 3). After 24-hour incubation, there were low fluorescence signals of the conjugates on the cell membrane and in the cytosol in all cell lines similar to those after 1-hour incubation. However, the conjugates were taken up into endo/lysosomes significantly more in all the cell lines studied as compares to those after 1-hour incubation ($P < 0.05$) (Fig. 3), although no statistical differences were found among the cell lines ($P > 0.05$). These results are in agreement with the EGFR expression and conjugate binding assay in the various cell lines.

TABLE 1. Binding affinity (Kd)

Cell line	Kd (nM) ± SD
A431	2.4 ± 0.09
OSC-19	0.4 ± 0.09
Scc-U2	0.2 ± 0.04
Scc-U8	0.3 ± 0.06

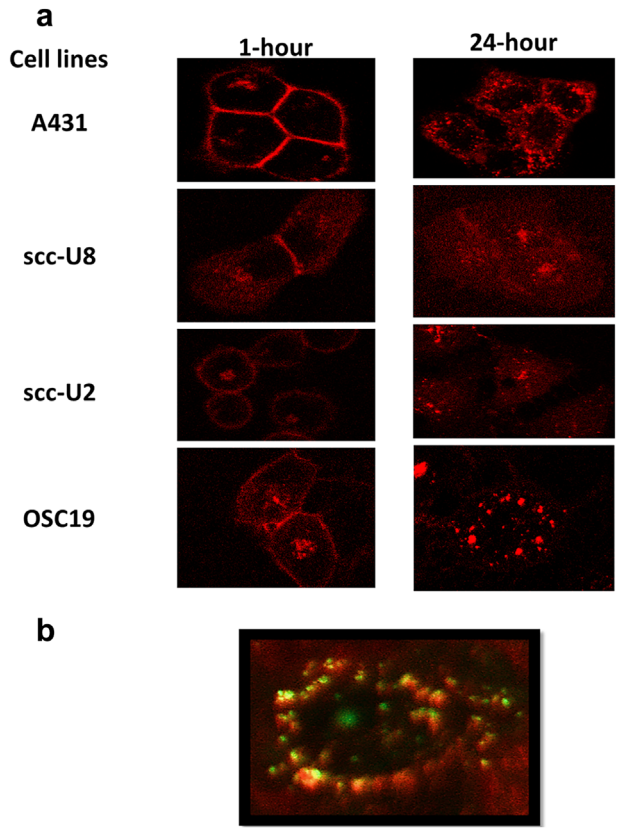

Fig. 2. Subcellular localization patterns of the conjugates in the A431, scc-U8, and scc-U2 and OSC19 cell lines (**a**). The localization pattern of LysoTracker (green fluorescence), an endo/lysosomal probe, was also studied after its co-incubation with the conjugates (red fluorescence) in the cell lines (**b**). The fluorescence images were made by the confocal laser scanning microscopy.

Dark Cytotoxicity of Cetuximab and Cetuximab-IR700DX Conjugates

No cytotoxicity was found in the MTS assay after incubating Cetuximab with A431, scc-U8, scc-U2, and OSC19 cell lines at various concentrations up to 2,000 μgml^{-1} for 24 hours (data not shown). In addition, no dark cytotoxicity was found with the MTS assay after incubating the Cetuximab-IR700DX conjugates with the same cell lines at various concentrations up to 2,000 μgml^{-1} for 24 hours (data not shown).

PIT Treatment With the Conjugates

Figure 4a shows the effect of PIT using different concentrations of the conjugates up to 100 μgml^{-1} for 1- or 24-hour incubation determined by the MTS cell proliferation assay. A dramatic decrease in cell proliferation was seen at the concentration of only 10 μgml^{-1} conjugates for 1-hour incubation in the A431 and scc-U8 cell lines. No killing effects on the scc-U2 and OSC19 cell lines were seen after the PIT treatment even at the 100 μgml^{-1} conjugates ($P < 0.05$ for all respective concentrations between A431 or scc-U8 and scc-U2 or OSC19 cell lines). Scc-U8 showed a decrease in cell proliferation with increased concentrations of conjugates after 24-hour incubation compared to 1-hour incubation. A431, scc-U2, and OSC19 had similar PIT results after a 24-hour incubation of the conjugates compared to the 1-hour incubation. Considering the clinical importance of the 24-hour drug light interval, the PIT effect was evaluated using the alamarBlue assay for a limited subset of treatment parameters. Figure 4b shows *ca.* 45% more PIT effect with scc-U2 and OSC19 cell lines determined with the alamarBlue compared to MTS assay. Both MTS and alamarBlue assay show significantly less response to PIT in the scc-U2 and OSC19 cell lines compared to the scc-U8 and A431 cell lines.

Mode of Cell Death After PIT With Cetuximab-IR700DX

The A431 and scc-U2 cell lines were selected to study the mode of cell death because the A431 cell line was very sensitive to targeted PIT due to its high EGFR expression; whereas the scc-U2 cell line was less sensitive to the same

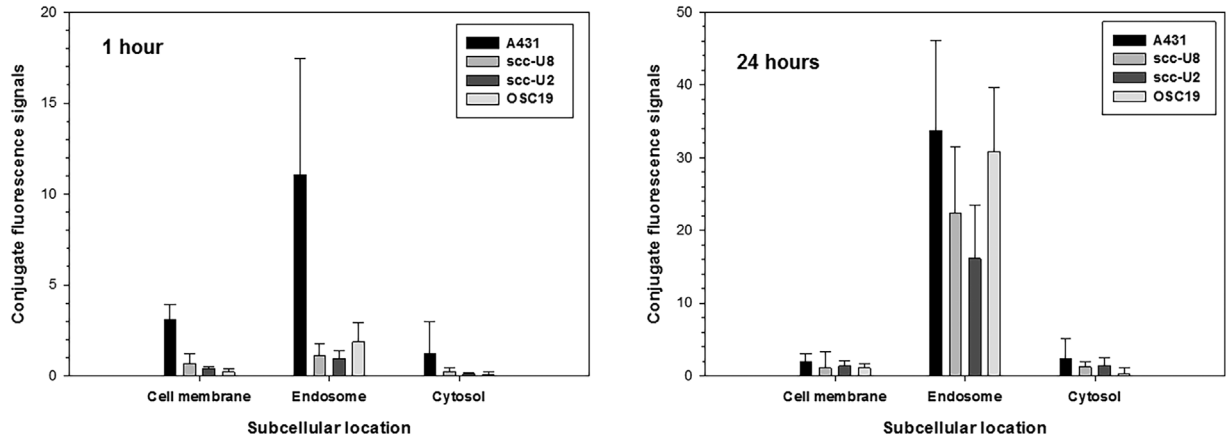

Fig. 3. Quantitative image analyses of various subcellular locations of the A431, scc-U8, scc-U2, and OSC19 cell lines incubated with the conjugates (40 μgml^{-1}) for 1- or 24-hour incubation.

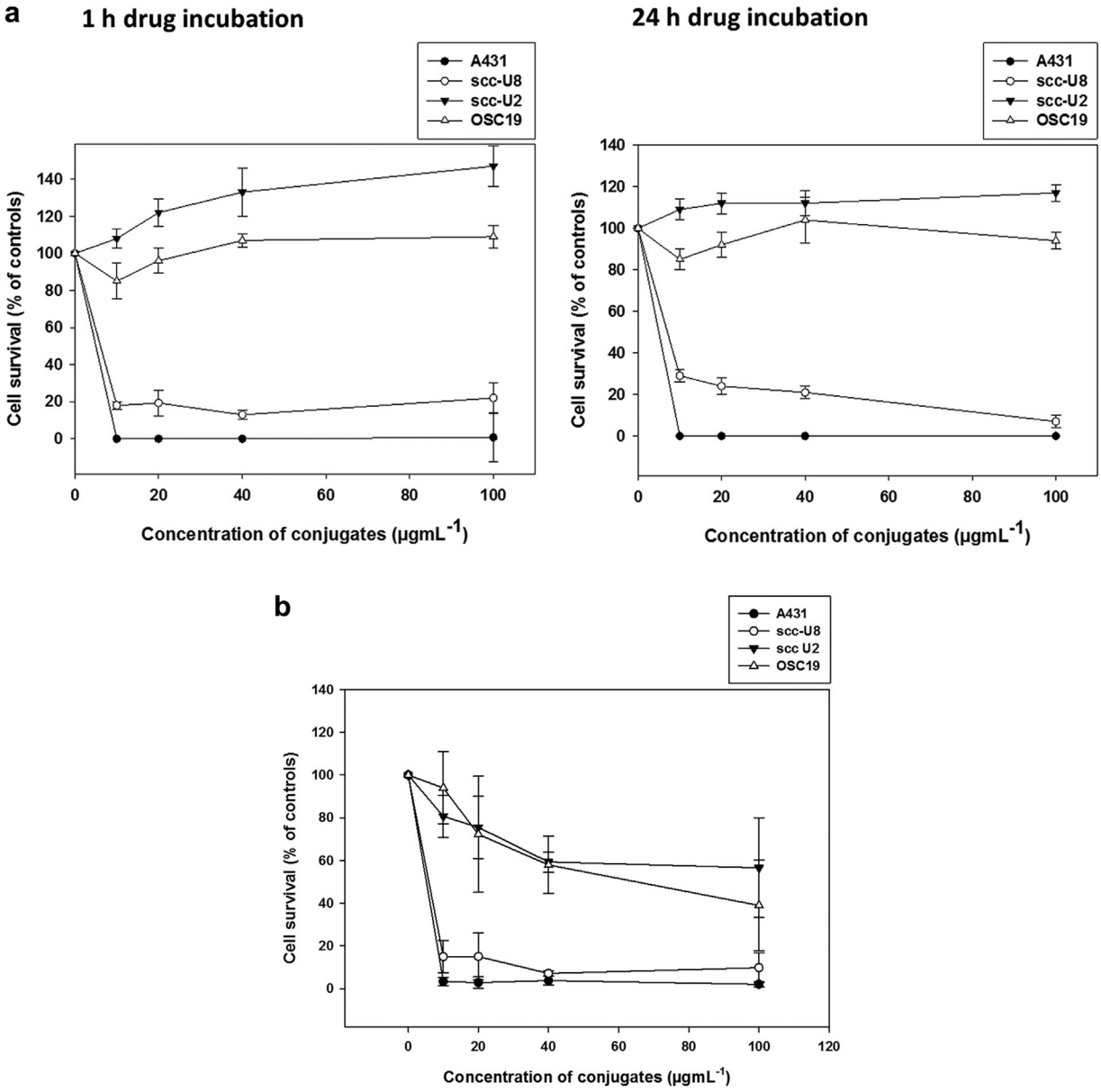

Fig. 4. Cell survivals of A431, scc-U8, scc-U2, and OSC19 cell lines at 24 hours after 1- or 24-hour incubation with the conjugates of Cetuximab and IR700DX at various concentrations (as indicated) before being irradiated with a 690 nm laser (5 $mW.cm^{-2}$, 7 $J.cm^{-2}$). The cell proliferation and viability were measured by the MTS assay (**a**) and alamarBlue assay (**b**), 24-hour incubation with the conjugates). Each data point represents the mean of at least three separate experiments with at least five individual samples per experiment. The bars are SD.

treatment. Figure 5 shows that for the cells that could be interrogated using flow-cytometry, approximately 13% were in early apoptosis and 37% were in late apoptosis 4 hours after the targeted PIT with 1-hour incubation of the conjugates in the A431 cells. At 48 hours after the treatment 23% were in early apoptosis and 67% were in late apoptosis, indicating that targeted PIT led largely to late apoptosis of A431 cells. Similar results were found in the targeted PIT treatment with 24-hour incubation of the conjugates in the cells. However, in the case of scc-U2 cell line, only approximately 1% were in early apoptosis and 2% were in late apoptosis 4 and 48 hours after the targeted PIT with 1-hour incubation. Targeted PIT treatment with 24-hour incubation of the conjugates showed 1% of cells in early apoptosis and 4% of cells in late apoptosis at 4 hours and 5% in early apoptosis and 17% in late apoptosis at 48 hours post treatment, respectively; clearly showing the cells less sensitive to the targeted PIT treatment.

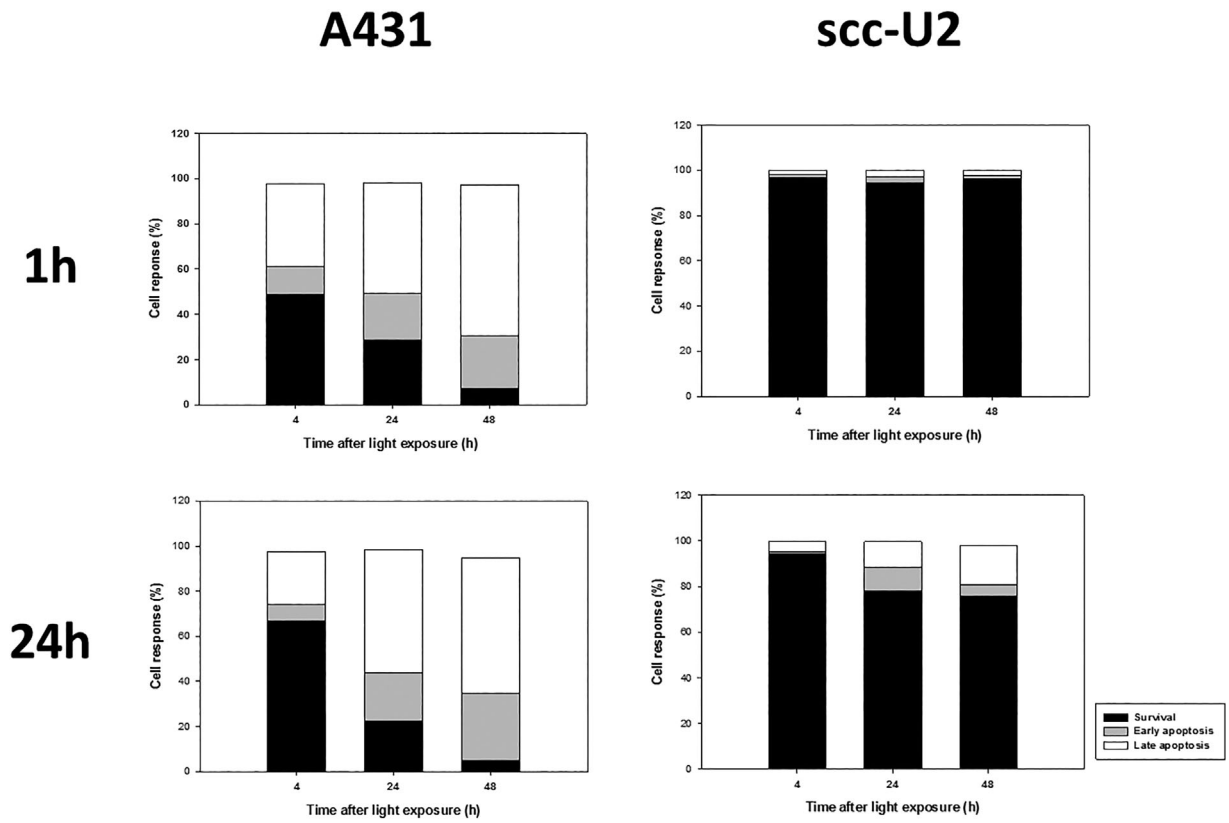

Fig. 5. Apoptosis/necrosis of the A431 and scc-U2 at 4-, 24-, and 48-hour after the targeted PIT with 1- or 24-hour incubation of the conjugates. The apoptosis/necrosis was measured with flow cytometry using Annexin V/propidium iodide staining.

Immunoblots of Anti-Apoptotic Proteins

The cell lines scc-U8 and scc-U2 were selected to study the difference in expression of anti-apoptotic proteins because they had a similar EGFR expression, but the scc-U2 was less sensitive to targeted PIT effect than scc-U8. Figure 6A shows the expression of proteins Bcl-2 and Bcl-xL in the scc-U8 and scc-U2 cell lines; while (B) presents the Bcl-2/beta actin ratio and Bcl-xL/beta actin ratio in the two cell lines. Although there are different degrees of expression of Bcl-2 and Bcl-xL in the cell lines, scc-U2 cells have significantly higher ratios of both Bcl-2/beta actin and Bcl-xL/beta actin than scc-U8 cell lines ($P < 0.05$), suggesting that scc-U2 cells are more resistant to apoptotic death than scc-U8, since both Bcl-2 and Bcl-xL are anti-apoptotic proteins.

DISCUSSION

The efficacy of targeted Cetuximab-IR700DX utilizing cell surface receptor, EGFR, is thought to be dependent on receptor density and to be mediated through a necrotic cell death pathway caused by the action of reactive oxygen species on the outer cell membrane [6,10,22]. Cells that express high levels of EGFR should be more sensitive to PIT than the cells with low levels of EGFR expression, which also serves as a protection for normal tissues expressing EGFR The present study shows that this is an over-simplification. Targeted PIT efficacy is likely not only related to the receptor density, but also to a more complicated mechanism of cell death than that associated with necrosis at the cell membrane. Although there are no previous studies showing this in targeted PIT, there are numerous mechanisms involved in the resistance to regular PDT treatments, ranging from the morphogical alterations of the cells to different levels of various protein expressions in individual cell lines [18].

The Cetuximab-IR700DX conjugate was localized on the cell membrane and in endo/lysosomes in A431 cells and PIT resulted in effective cell kill. However, scc-U8 and scc-U2 have a similar level of EGFR expression, with subsequent localization of Cetuximab-IR700DX on the cell membrane, but responded significantly differently. Scc-U8 were easily killed but the scc-U2 cells were less sensitive to the treatment with the light dose and fluence rate as applied in this study. In addition, OSC19 cells expressed a slightly higher level of EGFR than scc-U8 and scc-U2 and showed also a limited response. It has been shown that different cell survival assays may show different responses, for example the MTT assay is known to be less sensitive than the alamar blue under certain treatment conditions [23]. However, it is not immediately clear why we have found a 45% difference in cell survival between each assay. In each case the experimental

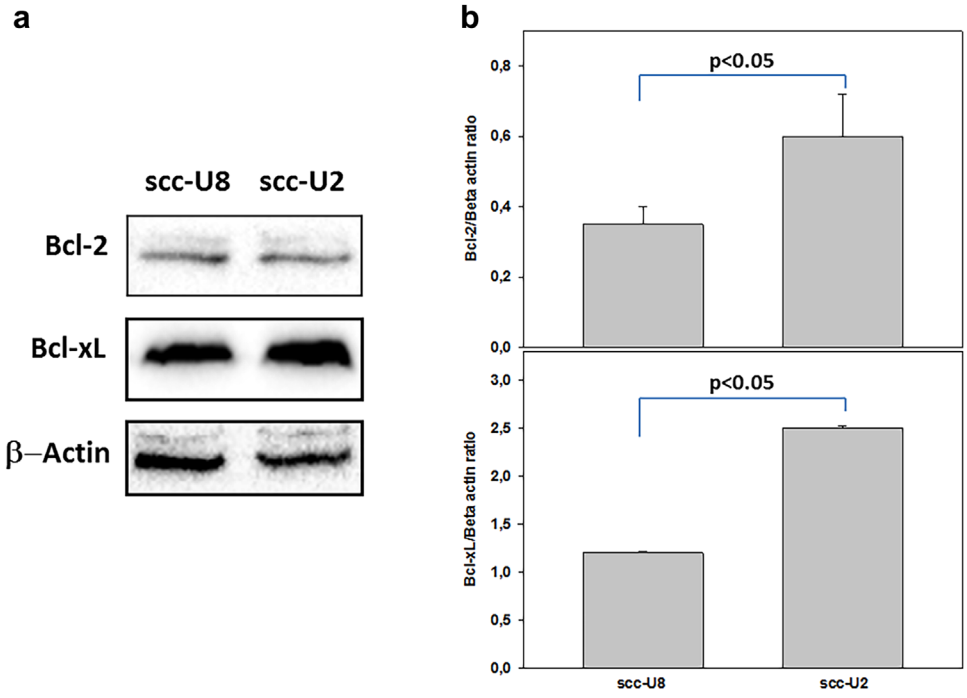

Fig. 6. (**a**) Expression of Bcl-2 and Bcl-xL in the scc-U8 and scc-U2 cell lines examined by immunoblots and the data are representative of three separate experiments. (**b**) Bcl-2/beta actin ratio and Bcl-xL/beta actin ratio in the two cell lines.

conditions were identical using the same batch of conjugate and PIT illumination protocol. Substantial decrease in cell survival of scc-U2 and OSC19 only occurred at higher fluences and fluence rates (data not shown). However, the fluence rate was intentionally kept at the low 5 mW.cm^{-2} in this study to avoid exhaustion of oxygen or induction of a hyperthermal effect (which has been described to occur for other photosensitizers in a similar context) [24,25].

Our results show that, in the case of OSC19 and ssc-U2 cell lines, there is no clear correlation between EGFR levels and targeted PIT-mediated cell death. This is not in agreement with the previous studies for example Heukers et al. [9] who demonstrated that PIT efficacy was correleated with the EGFR density of cells using EGFR targeted nanobodies. The reasons for this discrepancy are not known, but it might be explained by the use of different cell lines. It is also likely that nanobodies may interact differently with the cell membrane and cause a different balance of mechanisms of cell death compared to Cetuximab.

It is generally understood that the main cell death mechanism is induced by primary necrosis caused by damage to the outer cell membrane. After light exposure, the scc-U8 cells as well as A431 cells incubated with the conjugates were killed effectively. With flow cytometry using Annexin V/propidium iodide staining the mechanism of cell death was investigated, but it measures only fully intact cells and is therefore unable to detect small necrotic cell debris. Such exclusion of flow cytometric measurements may lead to underestimation of the fraction of cell death. Still, in the measurable fraction it is clear that cell death follows the apoptotic pathway. (Fig. 5). The sub-cellular localization plays an important role in the mechanism of cell death. Generally, hydrophobic sensitizers localize at the membraneous structures including plasma membrane, endoplasmic reticulum, mitochondria, nuclear membrane; while hydrophilic dyes mainly at the endo/lysosomes. These organelles are the initial targets of a photodynamic process, since the cytotoxic singlet oxygen produced by light-activated photosensitzer can only diffuse 10–20 nm during its very short lifetime [21]. Such initial PDT targets can be highly specific to trigger various signaling pathways of apoptotic induction. In this study the conjugate was found to be localized at the plasma membrane as well as endo/lysosomes after 1-hour and more in the endo/lysosomes after 24-hour incubation (Figs. 2a and 3) in all cell lines studied, particularly in A431. Several studies have shown that initial photodamage to plasma membrane or lysosomes can induce a marked delay or inhibition of apoptosis [26–28]. These effects may play a role in our study, since the conjugates initially localize mainly at the plasma membrane and later in the endo/lysosomes, destruction of these two locations after light exposure is expected. Furthermore, a relocalization of the photosensitizer during light irradiation has been hypothesized to cause photoinactivation of those enzymes required for the apoptotic process including the initiator caspases of 8 and 9 and effector caspases of 3, 6, and 7 [26]. However, the cell membrane/lysosomal

damage may induce apoptosis, but not through mitochondria-mediated apoptosis [29], a finding consistent with ours in the A431 cells (Fig. 5).

The Bcl-2 family of apoptosis proteins acts as a central decision maker in the apoptosis pathway. Cell lines that over-express Bcl-2 and Bcl-xL have been shown to be more resistant to PDT [29–32]. Chinese Hamster Ovary (CHO) cells transfected with an antiapoptotic protein gene have been shown to be more resistant to PDT [33]. Furthermore, overexpression of Bcl-2 can inhibit the activation-associated conformational change of the proapoptotic protein BAX [34]. Such results indicate that the extent of Bcl-2 expression may determine the sensitivity of tumor cells to apoptosis and to overall PDT-mediated cell killing [34]. In the present study, a significantly higher expression of Bcl-2 and Bcl-xL was found in the scc-U2 cells than scc-U8 cells (Fig. 6). This may explain the lower level of response of the scc-U2 cells to targeted PIT treatment.

It is important to stress that further studies are necessary to determine if these *in vitro* cellular effects are important *in-vivo*, first in pre-clinical tumor models and subsequently in clinical trials. The potential protective effect of anti-apoptotic proteins in some cells in head and neck tumors may result in variable PIT treatment responses.

In conclusion, although cellular expression and localization patterns of EGFR are similar in the three head and neck cell lines studied, Scc-U8 cell line is very sensitive to targeted PIT; while scc-U2 and OSC19 are not. The EGFR density does not seem to be the only determining factor for the different responses to PIT. We have shown for scc-U2 cells that the resistance of scc-U2 cells to PIT might be related to a lower degree of apoptotic induction due to a high expression of anti-apoptotic proteins of Bcl-2 and Bcl-xL.

ACKNOWLEDGMENTS

We would like to thank Erasmus Optical Imaging Center for their support with confocal imaging system, Departments of Surgical Oncology and Plastic and Reconstructive Surgery at Erasmus Medical Center for their cell-culture facilities and Aspyrian Therapeutics for providing Cetuximab-IR700DX.

REFERENCES

1. Dougherty TJ. Photodynamic therapy—new approaches. Semin Surg Oncol 1989;5:6–16.
2. Castano AP, Mroz P, Hamblin MR. Photodynamic therapy and anti-tumour immunity. Nat Rev Cancer 2006;6:535–545.
3. Allison RR, Moghissi K. Oncologic Photodynamic therapy: clinical strategies that modulate mechanisms of action. Photodiagnosis Photodyn Ther 2013;10:331–341.
4. Moan J, Steen HB, Feren K, Christensen T. Uptake of hematoporphyrin derivative and sensitized photoinactivation of C3H cells with different oncogenic potential. Cancer Lett 1981;14:291–296.
5. Mew D, Wat CK, Towers GH, Levy JG. Photoimmunotherapy: Treatment of animal tumors with tumor-specific monoclonal antibody-hematoporphyrin conjugates. J Immunol 1983;130:1473–1477.
6. Mitsunaga M, Ogawa M, Kosaka N, Rosenblum LT, Choyke PL, Kobayashi H. Cancer cell-selective in vivo near infrared photoimmunotherapy targeting specific membrane molecules. Nat Med 2011;17:1685–1691.
7. Study of RM-1929 and Photoimmunotherapy in patients with recurrent Head and Neck cancer, https://clinicaltrials.gov/ct2/show/NCT02422979?term=IRDye+700DX&rank=1
8. Sato K, Watanabe R, Hanaoka H, et al. Photoimmunotherapy: Comparative effectiveness of two monoclonal antibodies targeting the epidermal growth factor receptor. Mol Oncol 2014;8:620–632.
9. Heukers R, van Bergen en Henegouwen PM, Oliveira S. Nanobody-photosensitizer conjugates for targeted Photodynamic therapy. Nanomedicine 2014;10:1441–1451.
10. Kerr JF, Wyllie AH, Currie AR. Apoptosis: A basic biological phenomenon with wide ranging implication in tissue kinetics. Br J Cancer 1972;26:239–257.
11. Wyllie AH, Kerr JF, Currie AR. Cell death: The significance of apoptosis. Int Rev Cytol 1980;68:251–306.
12. Poon CKH, Hulett MD, Parish CR. Cell Death Differ 2010;17:381–397.
13. Chinnaiyan AM, O'Rourke K, Tewari M, Dixit VM. FADD, a novel death domain containing protein, interacts with the death domain of Fas and initiates apoptosis. Cell 1995;81:505–512.
14. Hus H, Xiong J, Goeddel DV. The TNF receptor 1-associated protein TRADD signals cell death and NF-Kappa B activation. Cell 1995;81:495–504.
15. Kroemer G. Mitochondral control of apoptosis: An introduction. Biochem Biophys Res Commun 2003;304:433–435.
16. Czabotar PE, Lessene G, Strasser A, Adams JM. Control of apoptosis by the BCL-2 protein family: Implications for physiology and therapy. Nat Rev Mol Cell Biol 2014;15:49–63.
17. Oleinick NL, Morris RL, Belichenko I. The role of apoptosis in response to photodynamic therapy: What, where, why, and how. Photochem Photobiol Sci 2002;1:1–21.
18. Casas A, Di Venosa G, Hasan T, Batlle Al. Mechanisms of resistance to photodynamic therapy. Curr Med Chem 2011;18:2486–2515.
19. Siddiqui MR, Railkar RS, Sanford T, Choyke PL, Kobayashi H, Agarwal PK. Targeting epidermal growth factor receptor (EGFR) and human epidermal growth factor receptor 2 expressing bladder cancer using combination photoimmunotherapy (PIT). J Clin Oncol 2017;35:15.
20. Kurai J, Chikumi H, Hashimoto K, et al. Antibody-dependent cellular cytotoxicity mediated by cetuximab against lung cancer cell lines. Clin Cancer Res 2007;13:1552–1561.
21. Moan J, Berg K. The photodegradation of porphyrins in cells can be used to estimate the lifetime of singlet oxygen. Photochem Photobiol 1991;53:549–553.
22. Zhang S, Jia N, Shao P, Tong Q, Xie XQ, Bai M. Target-selective phototherapy using a ligand-based photosensitizer for type 2 cannabinoid receptor. Chem Biol 2014;21:338–344.
23. Hamid R, Rotshteyn Y, Rabadi L, Parikh R, Bullock P. Comparison of alamar blue and MTT assays for high throughput screening. Toxicol In Vitro 2004;18:703–710.
24. Rijcken CJ, Hofman JW, van Zeeland F, Hennink WE, van Nostrum CF. Photosensitiser-loaded biodegradable polymeric micelles: Preparation, characterisation and *in vitro* PDT efficacy. J Control Release 2007;124:144–153.
25. Hofman JW, Carstens MG, van Zeeland F, Helwig C, Flesch FM, Hennink WE, van Nostrum CF. Photocytotoxicity of mTHPC (temoporfin) loaded polymeric micelles mediated by lipase catalyzed degradation. Pharm Res 2008;25:2065–2073.
26. Moor AC. Signaling pathways in cell death and survival after Photodynamic therapy. J Photochem Photobiol B 2000;57:1–13.
27. Kessel D. Relocalization of cationic porphyrins during Photodynamic therapy. Photochem Photobiol Sci 2002;1:837–840.
28. Kessel D, Castelli M. Evidence that Bcl-2 is the target of three photosensitizers that induce a rapid apoptotic response. Photochem Photobiol 2001;74:318–322.
29. Shen XY, Zacal N, Singh G, Rainbow AJ. Alterations in mitochondrial and apoptosis-regulating gene expression in Photodynamic therapy-resistant variants of HT29 colon carcinoma cells. Photochem Photobiol 2005;81:306–313.

30. Granville DJ, Jiang H, An MT, Levy JG, McManus BM, Hunt DW. Bcl-2 overexpression blocks caspase activation and downstream apoptotic events instigated by Photodynamic therapy. Br J Cancer 1999;79:95–100.
31. Usuda J, Hirata T, Ichinose S, et al. Tailor-made approach to Photodynamic therapy in the treatment of cancer based on Bcl-2 photodamage. Int J Oncol 2008;33:689–696.
32. Ichinose S, Usuda J, Hirata T, et al. Lysosomal cathepsin initiates apoptosis, which is regulated by photodamage to Bcl-2 at mitochondria in Photodynamic therapy using a novel photosensitizer. ATX-s10 (Na). Int J Oncol 2006;29:349–355.
33. He J, Agarwal M, Larkin H, Friedman L, Xue L, Oleinick N. The induction of partial resistance to Photodynamic therapy by the protooncogene BCL-2. Photochem Photobiol 1996;64:845–852.
34. Usuda J, Azizuddin K, Chiu SM, Oleinick NL. Association between the Photodynamic loss of Bcl-2 and the sensitivity to apoptosis caused by phthalocyanine Photodynamic therapy. Photochem Photobiol 2003;78:1–8.